

Supporting Information

Synthetic Control of the Polar Units in the Poly(thiophene carbazole) Porous Networks for Effective CO₂ Capture

Chan Yao,^a Di Cui,^a Yiang Zhu,^b Wei Xie,^a Shuran Zhang,^a Guangjuan Xu,^a and Yanhong Xu^{*a,c}

^a Key Laboratory of Preparation and Applications of Environmental Friendly Materials (Jilin Normal University), Ministry of Education, Changchun, 130103, China.

^b School of Environmental Studies, China University of Geosciences, Lumo Road 388, Wuhan, Hubei Province, China.

^c School of Chemistry and Environmental Engineering, the Collaborative Innovation Center of Optical Materials and Chemistry, Changchun University of Science and Technology, Changchun, 130022, China.

* Corresponding Author. Email: xuyh198@163.com

Contents

Section A. Materials and methods

Section B. Synthetic procedures

Section C. FT-IR spectra

Section D. The Solid-UV spectra

Section E. TEM images

Section F. XPS spectrum

Section G. Powder X-ray diffraction patterns

Section H. TGA curves

Section I. CO₂, CH₄ and N₂ gas adsorption isotherms

Section J. Selectivity analyses

Section A. Materials and methods

1,4-Benzene diboronic acid, 2,5-dibromothiophene-3-carboxylic acid, 1,3,6,8-tetrabromocarbazole and tetrakis(triphenylphosphine)palladium (0) were purchased from Alfa. Potassium carbonate was purchased from Energy chemical. All solvents used were purchased from Aladdin.

¹H NMR spectra were recorded on Bruker AvanceIII models HD 400 NMR spectrometers, where chemical shifts (δ in ppm) were determined with a residual proton of the solvent as standard. Fourier transform Infrared (FT-IR) spectra were recorded on a Perkin-elmer model FT-IR-frontier infrared spectrometer. The solution UV-visible analyzer was used for shimadzu UV-3600. The holder with solid samples of CMPs in KBr pellets was mounted onto the window of the integration sphere. X-ray photoelectron spectra (XPS) were recorded on an ESCALAB250Xi electron spectrometer (Thermo Fisher Scientific Inc., Waltham, MA, USA). Field-emission scanning electron microscopy (FE-SEM) images were performed on a JEOL model JSM-6700 operating at an accelerating voltage of 5.0 kV. High-resolution transmission electron microscopy (HR-TEM) images were obtained on a JEOL model JEM-3200 microscopy. Powder X-ray diffraction (PXRD) data were recorded on a Rigaku model RINT Ultima III diffractometer by depositing powder on glass substrate, from $2\theta = 1.5^\circ$ up to 60° with 0.02° increment. TGA analysis was carried out using a Q5000IR analyser (TA Instruments) with an automated vertical overhead thermobalance. Before measurement, the samples were heated at a rate of 5°C min^{-1} under a nitrogen atmosphere.

Nitrogen sorption isotherms were measured at 77 K with ASIQ (iQ-2) volumetric adsorption analyzer. Before measurement, the samples were degassed in vacuum at 120°C for more than 10 h. The Brunauer-Emmett-Teller (BET) method was utilized to calculate the specific surface areas and pore volume. The Saito-Foley (SF) method was applied for the estimation of pore size and pore size distribution.

Carbon dioxide, methane and nitrogen sorption isotherms were measured at 273 K or 298 K with a Bel Japan Inc. model BELSORP-max analyzer, respectively. Before measurement, the samples were also degassed in vacuum at 120°C for more than 10 h.

Section B. Synthetic procedures

Synthesis of SN@CMP-1

To a mixture of 1,4-benzene diboronic acid (BDA, 331.8 mg, 2 mmol) and 2,5-dibromothiophene-3-carboxylic acid (DBrTA, 572 mg, 2 mmol) in dimethylformamide (DMF, 20 mL), an aqueous solution of K_2CO_3 (2.0 M, 1.5 mL) and tetrakis(triphenylphosphine)palladium (0) (25 mg, 21.6 μ mol) were added. The mixture was degassed and purged with N_2 , and stirred at 150 °C for 48 h. The mixture was cooled to room temperature and poured into methanol. The precipitate was collected by filtration, and washed with H_2O , $CHCl_3$, THF and acetone sequentially. Further purification of the polymer was carried out by Soxhlet extraction with THF for 24 h. The product was dried in vacuum for 24 h at 70 °C and obtained as a fine green powder (yield: 254 mg, 57.7%). Elemental combustion analysis (%) calcd for $C_{22}H_{12}O_4S_2$ (based on the theoretical formula for an infinite SN@CMP-1 network without any unreacted end group): C 65.35, H 2.97, S 15.86; found: C 63.08, H 4.85, S 13.55.

Synthesis of SN@CMP-2

BDA (331.8 mg, 2 mmol), DBrTA (457.6 mg, 1.6 mmol) and 1,3,6,8-tetrabromocarbazole (TBrCz, 96.6 mg, 0.2 mmol) were used in this polymerization (yield: 82.5%), details as described for SN@CMP-1. Elemental combustion analysis (%) calcd for $(C_{22.4}H_{10.2}O_{3.2}S_{1.6}N_{0.2})_n$: C 69.96, H 2.65, S 13.34, N 0.73; found: C 66.35, H 3.24, S 10.80, N 1.29.

Synthesis of SN@CMP-3

BDA (331.8 mg, 2 mmol), DBrTA (343.2 mg, 1.2 mmol) and TBrCz (193.2 mg, 0.4 mmol) were used in this polymerization (yield: 83.5%), details as described for SN@CMP-1. Elemental combustion analysis (%) calcd for $(C_{22.8}H_{12.4}O_{2.4}S_{1.2}N_{0.4})_n$: C 74.27; H 3.36, S 10.43, N 1.52; found: C 70.43; H 2.98, S 9.13, N 1.35.

Synthesis of SN@CMP-4

BDA (331.8 mg, 2 mmol), DBrTA (286 mg, 1 mmol) and TBrCz (241.4 mg, 0.5 mmol) were used in this polymerization (yield: 85.9%), details as described for SN@CMP-1. Elemental combustion analysis (%) calcd for $(C_{23}H_{12.5}O_2S_1N_{0.5})_n$: C 76.78; H 3.47, S 8.91, N 1.95; found: C 71.23; H 2.68, S 8.05, N 2.07.

Synthesis of SN@CMP-5

BDA (331.8 mg, 2 mmol), DBrTA (228.8 mg, 0.8 mmol) and TBrCz (289.6 mg, 0.6 mmol) were used in this polymerization (yield: 83.7%), details as described for SN@CMP-1. Elemental combustion analysis (%) calcd for $(C_{23.2}H_{12.6}O_{1.6}S_{0.8}N_{0.6})_n$: C 79.41; H 3.59, S 7.31, N 2.39; found: C 80.15; H 2.92, S 6.87, N 3.01.

Synthesis of SN@CMP-6

BDA (331.8 mg, 2 mmol), DBrTA (114.4 mg, 0.4 mmol) and TBrCz (386.2 mg, 0.8 mmol) were used in this polymerization (yield: 82.3%), details as described for SN@CMP-1. Elemental combustion analysis (%) calcd for $(C_{23.6}H_{12.8}O_{0.8}S_{0.4}N_{0.8})_n$: C 85.10; H 3.84, S 3.85, N 3.36; found: C 81.33; H 3.20, S 3.06, N 2.70.

Synthesis of SN@CMP-7

BDA (331.8 mg, 2 mmol) and TBrCz (483 mg, 1 mmol) were used in this polymerization (yield: 85.4%), details as described for SN@CMP-1. Elemental combustion analysis (%) calcd for $(C_{24}H_{13}N)_n$:

C 91.4, H 4.15, N 4.44; found: C 87.81; H 4.59; N 3.40.

Section C. FT-IR spectra

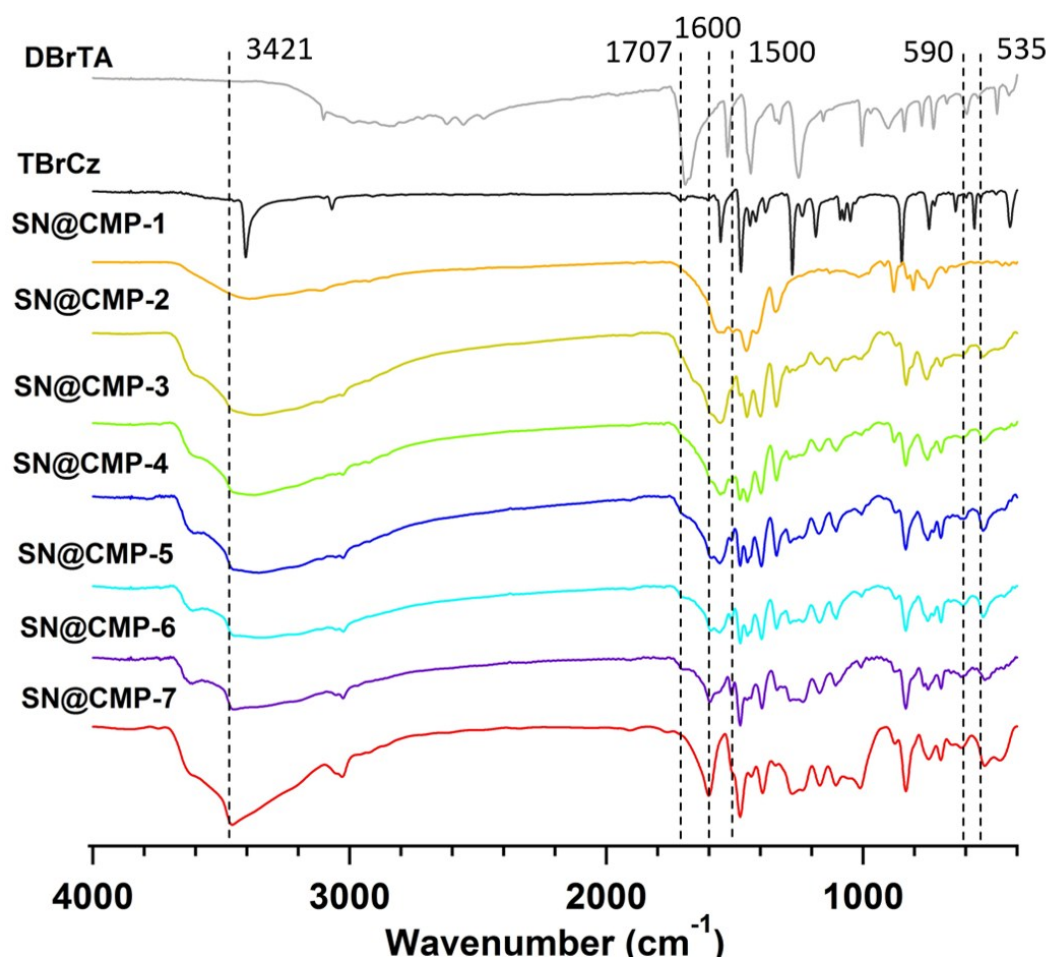


Figure S1. FT-IR spectra of 2,5-dibromothiophene-3-carboxylic acid (DBrTA), 1,3,6,8-tetrabromocarbazole (TBrCz), and copolymers SN@CMP-1-7 networks.

Section D. The Solid-UV spectra

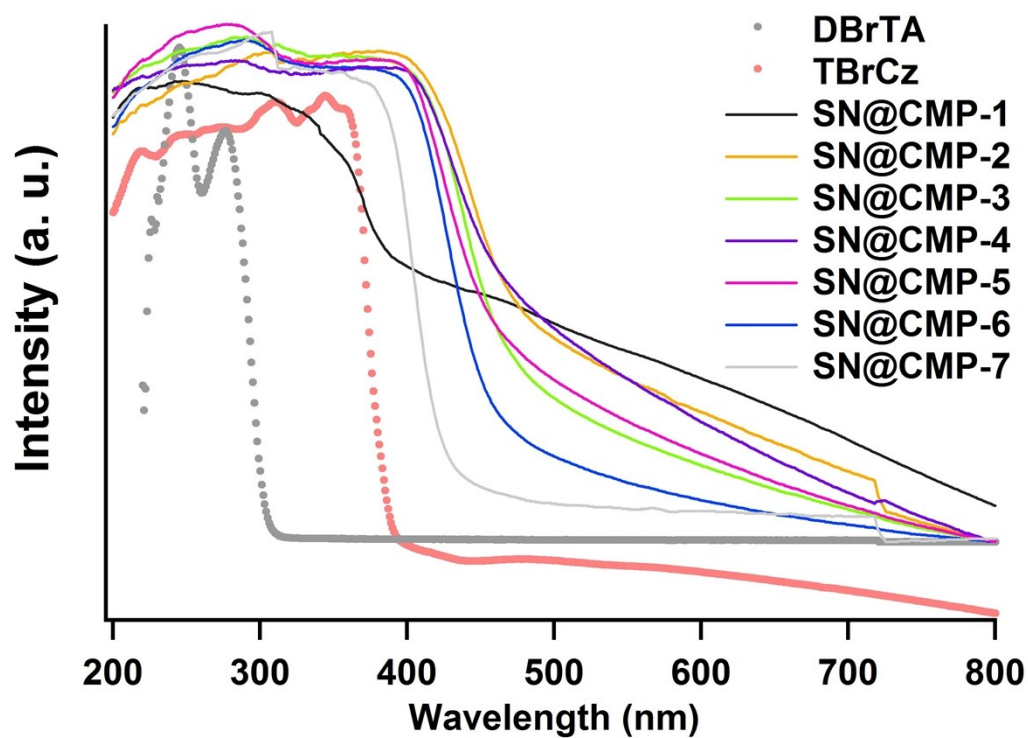


Figure S2. Electronic absorbance spectra of copolymer SN@CMP1-7 in the solid state.

Section E. TEM images

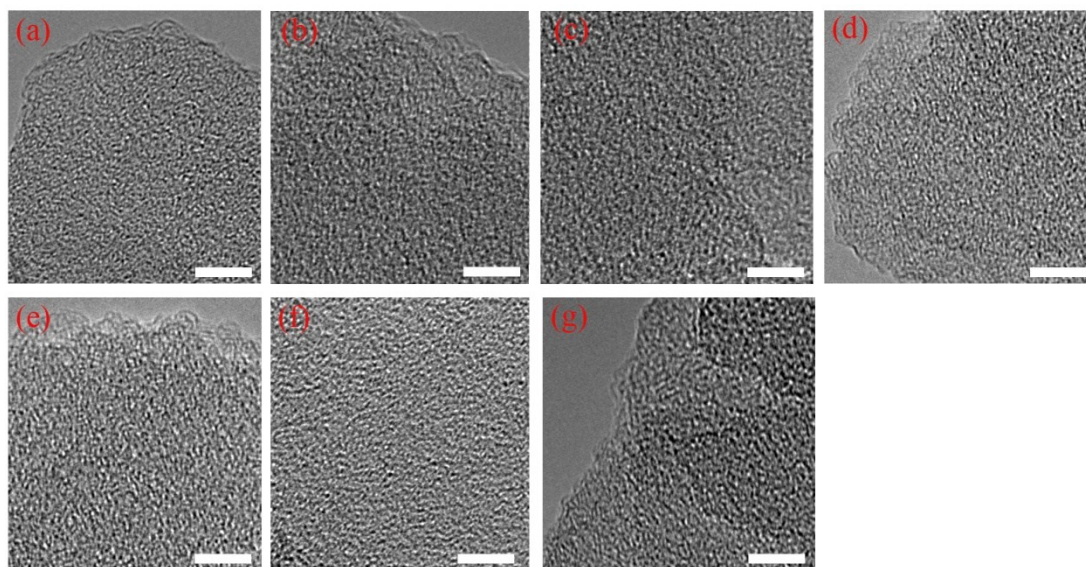


Figure S3. TEM images of the copolymer networks (a) SN@CMP-1, (b) SN@CMP-2, (c) SN@CMP-3, (d) SN@CMP-4, (e) SN@CMP-5, (f) SN@CMP-6, and (g) SN@CMP-7 (5 nm width).

Section F. XPS spectrum

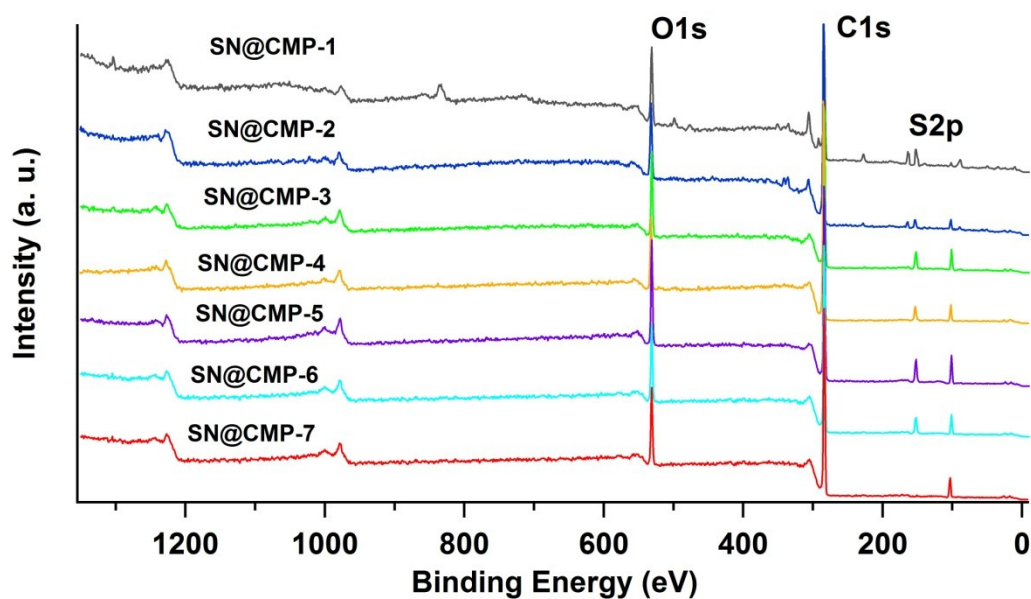


Figure S4. XPS survey spectrum of SN@CMP-1-7.

Section G. Powder X-ray diffraction patterns

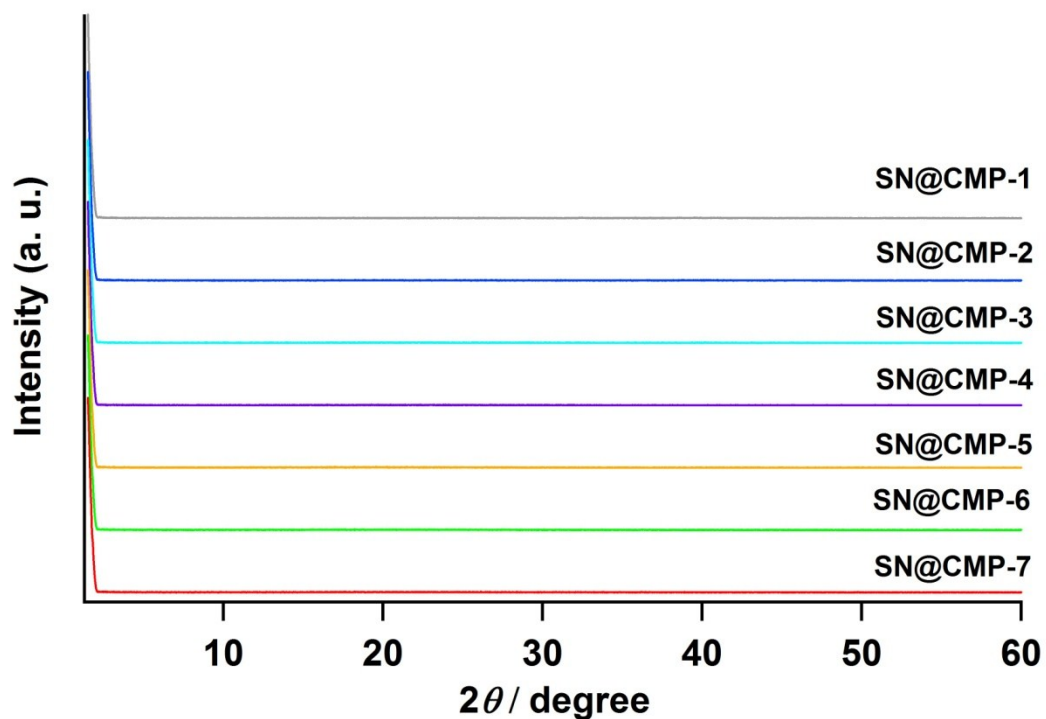


Figure S5. Powder X-ray diffraction profiles of copolymer networks SN@CMP-1-7.

Section H. TGA curves

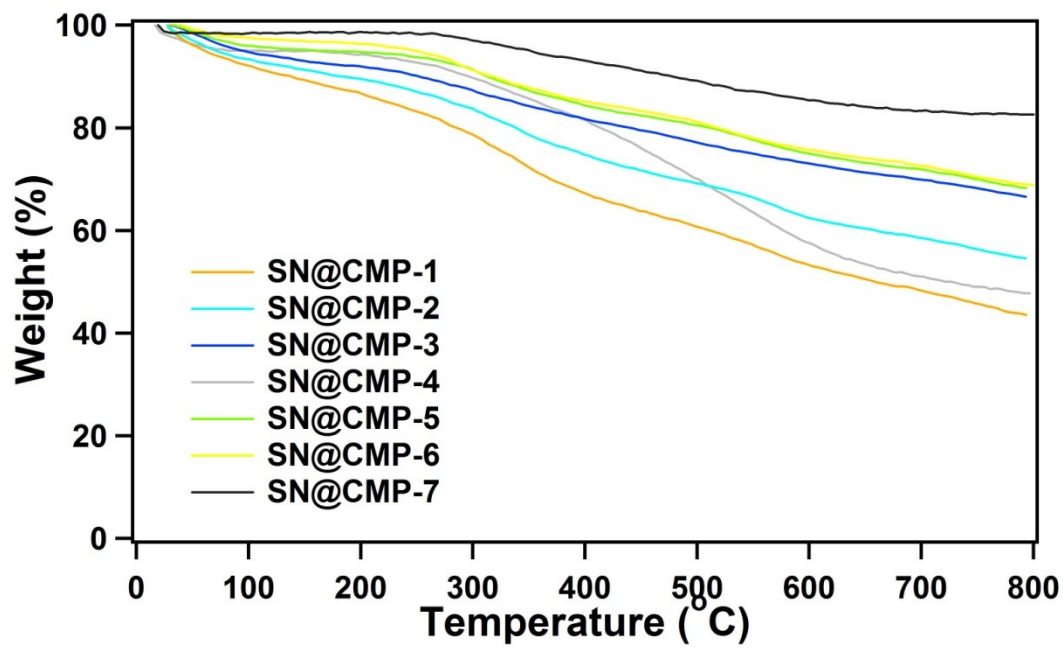


Figure S6. TGA curves of SN@CMP-1-7.

Section I. CO₂, CH₄ and N₂ gas adsorption isotherms

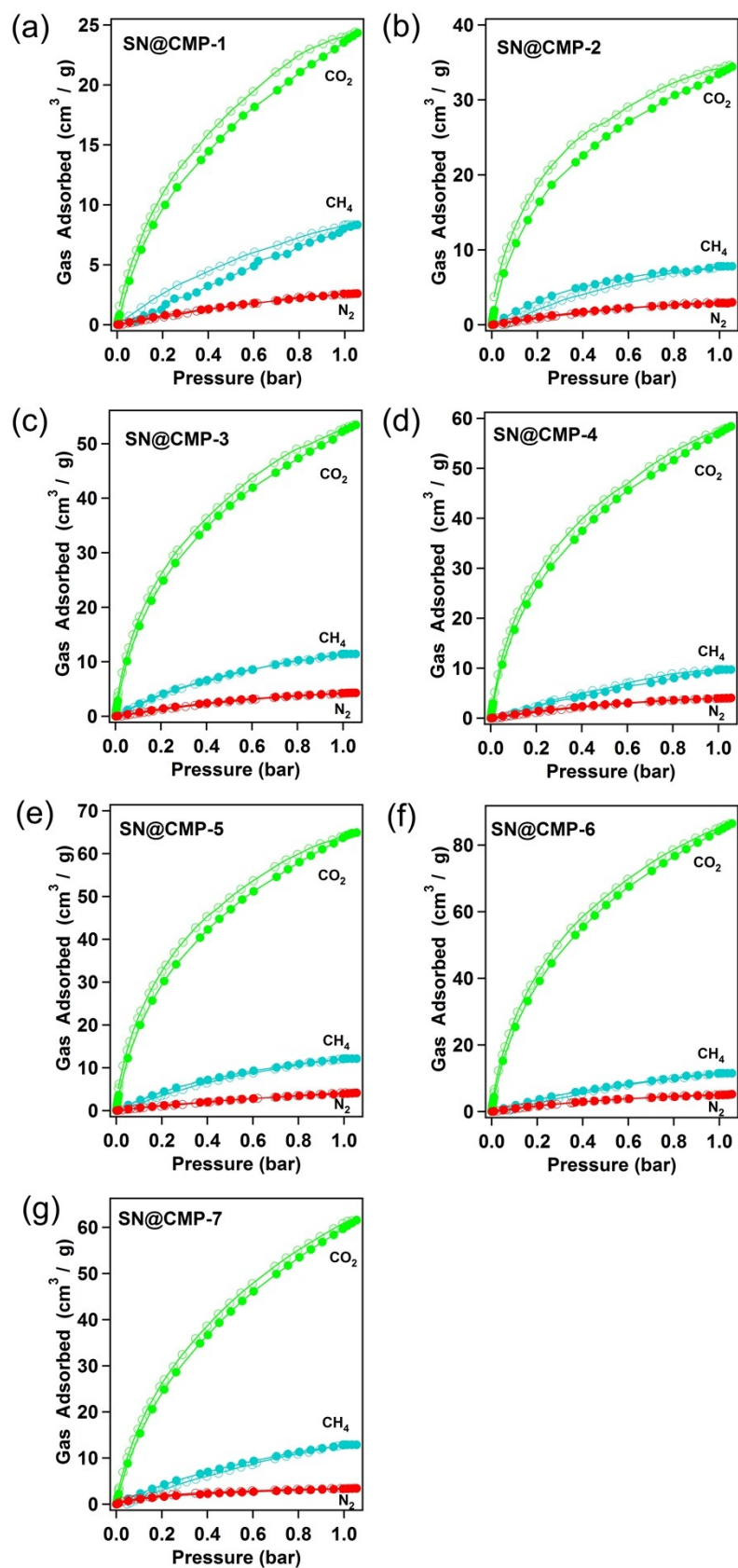


Figure S7. CO₂, CH₄ and N₂ gas adsorption isotherms collected at 1.05 bar and 273 K.

Section J. Selectivity analyses

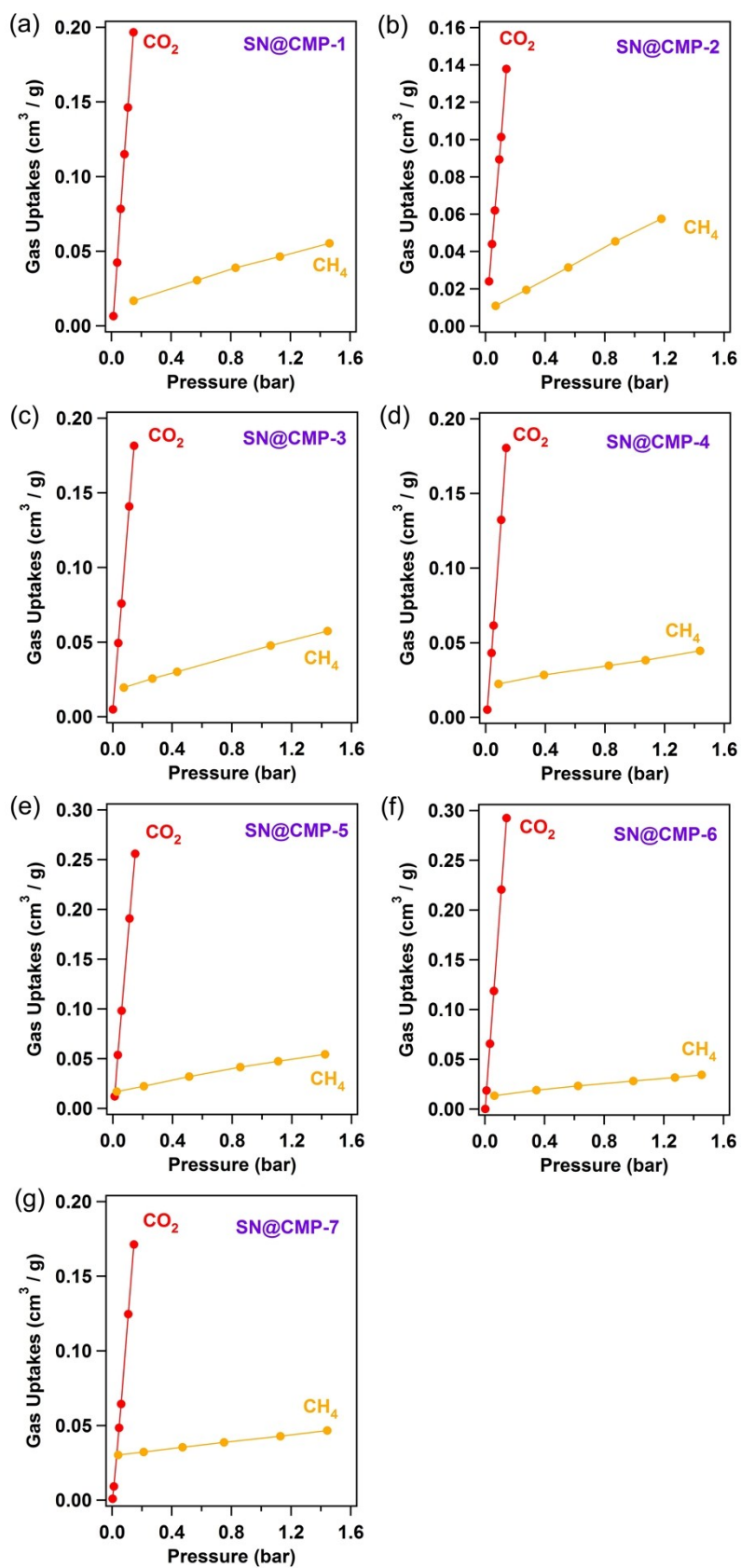


Figure S8. CO_2/CH_4 initial slope selectivity studies for SN@CMP-1-7 at 273 K and 1.05 bar.

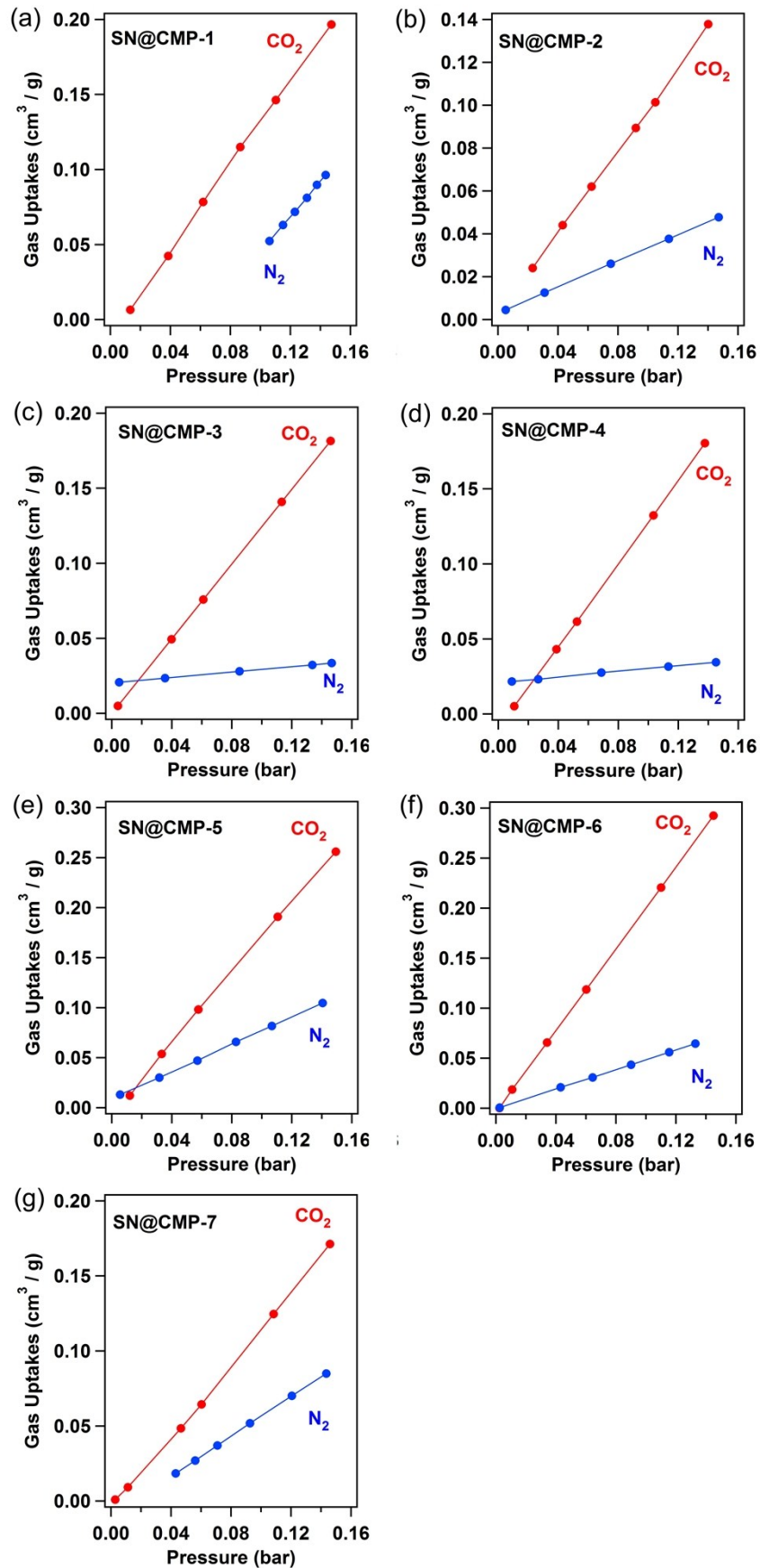


Figure S9. CO_2/N_2 initial slope selectivity studies for SN@CMP-1-7 at 273 K and 1.05 bar.

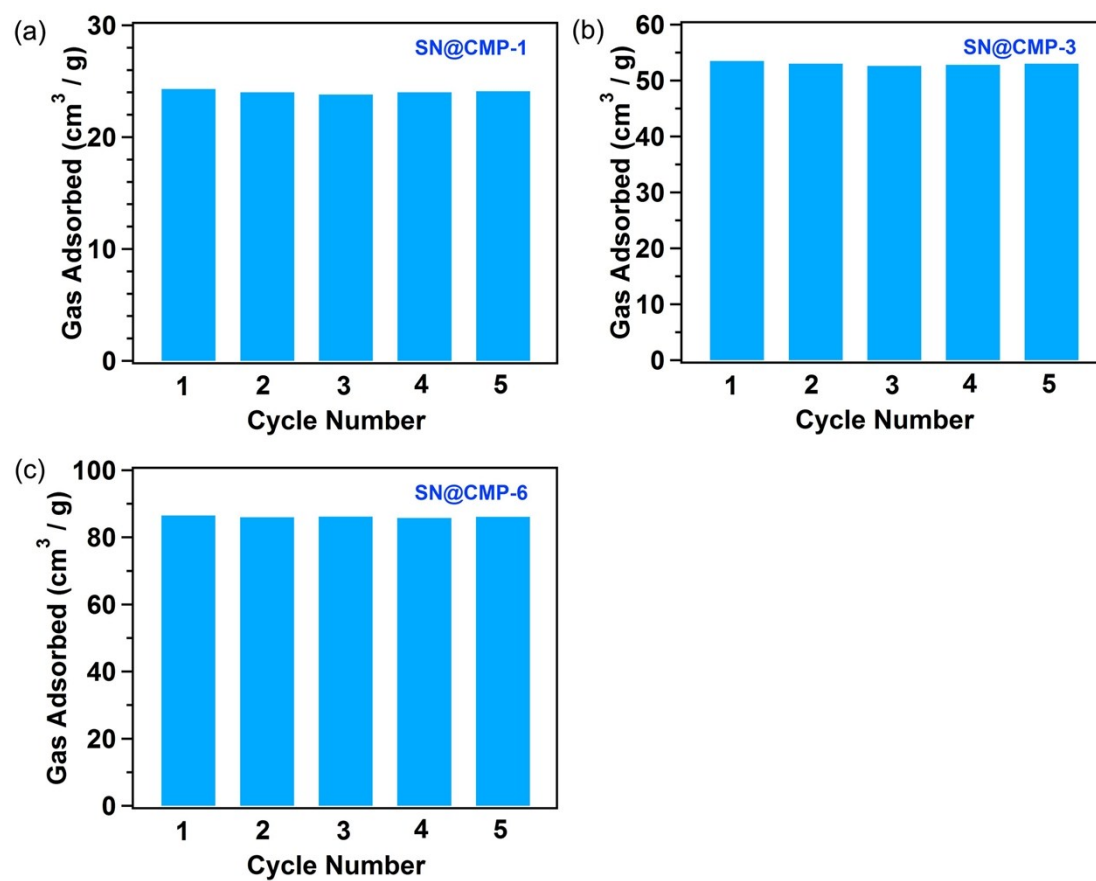
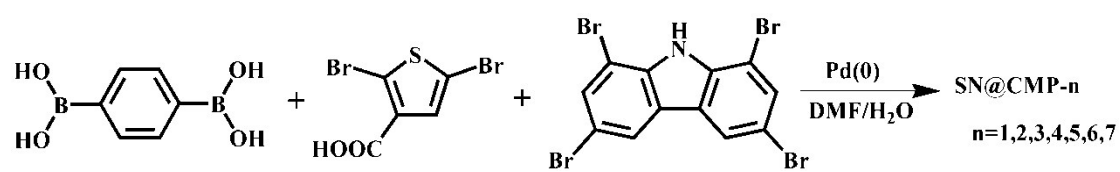
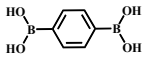
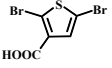
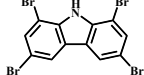


Figure S10. CO₂ reusability of the Poly(thiophene carbazole) CMPs.



Scheme S1. Synthetic route of copolymerization for SN@CMP-1-7.

Table S1. Copolymerization with different molar ratios of two halogen monomers.

Copolymers	 [mmol]	 [mmol]	 [mmol]	$S_{\text{BET}}^{\text{a}}$ [m ² g ⁻¹]	$S_{\text{Micro}}^{\text{b}}$ [m ² g ⁻¹]	$V_{\text{Total}}^{\text{c}}$ [cm ³ g ⁻¹]	$V_{\text{Micro}}^{\text{d}}$ [cm ³ g ⁻¹]
SN@CMP-1	2	2	0	89	19	0.12	0.02
SN@CMP-2	2	1.6	0.2	590	548	0.44	0.23
SN@CMP-3	2	1.2	0.4	804	626	0.78	0.38
SN@CMP-4	2	1.0	0.5	1143	885	1.04	0.62
SN@CMP-5	2	0.8	0.6	1356	1030	1.42	0.85
SN@CMP-6	2	0.4	0.8	1172	920	1.16	0.76
SN@CMP-7	2	0	1.0	804	596	0.80	0.54

^a Surface area calculated from the N₂ adsorption isotherm using the BET method. ^b Micropore surface area calculated from the N₂ adsorption isotherm using the *t*-plot method. ^c Total pore volume at $P/P_0 = 0.99$. ^d Micropore volume derived using the *t*-plot method based on the Halsey thickness equation.

Table S2. Summary of gas uptakes for the copolymer networks.

Copolymers	CO ₂ uptake ^a	CO ₂ uptake ^b	CH ₄ uptake ^c	N ₂ uptake ^d	Selectivity ^e	
	[cm ³ g ⁻¹]	[cm ³ g ⁻¹]	[cm ³ g ⁻¹]	[cm ³ g ⁻¹]	CO ₂ /CH ₄	CO ₂ /N ₂
SN@CMP-1	24.3	15.1	8.4	2.6	4.6	22.6
SN@CMP-2	34.4	23.8	7.8	2.9	7.7	27.7
SN@CMP-3	53.5	33.5	11.4	4.3	6.9	36.9
SN@CMP-4	58.4	38.1	9.8	4.6	6.0	38.0
SN@CMP-5	64.9	44.8	12.2	4.1	6.5	56.5
SN@CMP-6	86.5	53.4	11.4	5.2	4.5	61.5
SN@CMP-7	61	43.0	12.8	3.4	6.1	36.8

^a Data collected at 273 K and 1.0 bar. ^b Data collected at 298 K and 1.0 bar. ^{c,d} Data collected at 273 K and 1.0 bar. ^e Adsorption selectivity based on Henry's law.

Kinetics of CO₂ adsorption and desorption

To quantify the surfactant effect on the rate of the CO₂-adsorption processes, the kinetics of adsorption were analyzed by using the double-exponential kinetic model. According to this model, the mass of CO₂ adsorbed as a function of time is expressed by eq. 1:

$$\frac{M_t}{M_e} = A_S \left(1 - \exp(-k_S t) \right) + A_D \left(1 - \exp(-k_D t) \right) \quad \text{eq. 1}$$

In eq. 1, M_t and M_e represent the experimental mass gain due to CO₂ sorption at time t and after reaching equilibrium, respectively. The experimental M_e , M_t , and the time of adsorption (t) were fitted with eq. 1 by using the Sigma Plot 2012 software with a tolerance value set at 1×10^{-10} . As shown in eq. 1, there were four fitting parameters, namely, A_S , A_D , k_S , and k_D . A_S and A_D are defined as the relative contributions of the surface and diffusion barriers, respectively, controlling the overall adsorption process, in which the sum of A_S and A_D is equal to 1, and k_S and k_D are defined as the corresponding surface and diffusion rate constants, respectively.

CO₂ desorption obeyed the following first-order kinetic relationship:

$$M_{des} = M_o e^{-k_{des} t} \quad \text{eq. 2}$$

In which M_{des} is the mass of CO₂ desorbed at time t and M_o is the initial mass of previously adsorbed CO₂, i.e., the mass at maximum adsorption, and k_{des} is the desorption rate constant.

The relationship between the specific rate of desorption as a function of temperature is described by the Arrhenius equation as follows:

$$k_{des} = A e^{-\frac{E_a}{RT}} \quad \text{eq. 3}$$

In which A is the Arrhenius pre-exponential constant, E_a is the activation energy of desorption, R is the universal gas constant, and T is the temperature.

Calculations of adsorption selectivity

Adsorption selectivities can be calculated by a virial fitting method based on the following equation:

$$\ln N / P = A_0 + A_1 N + A_2 N^2 + A_3 N^3 + \dots \quad \text{eq. 4}$$

In eq. 4, P is pressure, N is amount adsorbed and A_0 , A_1 etc. present virial coefficients. A_0 is related to adsorbate–adsorbent interactions, and A_1 describes adsorbate–adsorbate interactions. The Henry's Law

constant (K_H) is equal to $\exp(A_\theta)$.

The Henry's Law selectivity for gas component i over j is calculated based on eq. 5:

$$S_{ij} = K_{Hi} / K_{Hj} \quad \text{eq. 5}$$